

AQ: A

High-Speed Interferometric Detection of Label-Free Immunoassays on the Biological Compact Disc

AQ: B

MING ZHAO,¹ DAVID NOLTE,^{1*} WONRYEON CHO,² FRED REGNIER,² MANOJ VARMA,³
GREG LAWRENCE,³ and JOHN PASQUA³

AQ: C **Background:** We describe a direct-detection immunoassay that uses high-speed optical interferometry on a biological compact disc (BioCD).

Methods: We fabricated phase-contrast BioCDs from 100-mm diameter 1.1-mm thick borosilicate glass disks coated with a 10-layer dielectric stack of Ta₂O₅/SiO₂ that serves as a mirror with a center wavelength at 635 nm. The final layer is a $\lambda/4$ layer of SiO₂ onto which protein patterns are immobilized through several different chemical approaches. Protein on the disc is scanned by a focused laser spot as the disc spins. Interaction of the light with the protein provides both a phase-modulated signal and a local reference that are combined interferometrically to convert phase into intensity. A periodic pattern of protein on the spinning disc produces an intensity modulation as a function of time. The binding of antigen or antibodies is detected directly, without labels, by a change in the interferometric intensity. The technique is demonstrated with a reverse assay of immobilized rabbit and mouse IgG antigen incubated against anti-IgG antibody in a casein buffer.

AQ: D

Results: The signal increased with increased concentration of analyte. The current embodiment detected a concentration of 100 ng/L when averaged over ~3000 100-micron-diameter protein spots.

Conclusions: High-speed interferometric detection of label-free protein assays on a rapidly spinning BioCD is

a high-sensitivity approach that is amenable to scaling up to many analytes.

© 2006 American Association for Clinical Chemistry

Highly multiplexed multianalyte immunologic assays favor label-free detection because no secondary reagents are needed. Direct optical detection senses the presence or absence of bound analyte as a change in detected intensity related to the mass density captured on the surface. Solid-support immunoassays based on optical detection enable small spot sizes that in principle could be scaled down to the size of the wavelength of light and hence have the advantage of large assay densities. For instance, a 100-mm-diameter disc has a surface area of 5 billion square wavelengths, providing the possibility for 5 billion measurements per disc. Optical interferometry also has extremely high sensitivity, with surface height accuracy down to subnanometer vertical resolution averaged over the size of the laser focal spot.

FN4

We introduced the biological compact disc (BioCD)⁴ to incorporate the advantages of direct optical detection into a sensitive and scalable immunoassay platform (1, 2). The 1st BioCD demonstration was related in structure to conventional optical compact discs, but rather than operating in digital mode, it was modified to operate in interferometric phase quadrature (3), in which the signal and reference beams have a 90° relative phase difference. We have extended interferometric quadrature to a fundamentally new class of BioCD, the phase-contrast class that has simple and inexpensive disc construction, simple detection optics, and significantly improved sensitivity.

AQ: E

Departments of ¹Physics and ²Chemistry, Purdue University, West Lafayette, IN.

³QuadraSpec Inc., West Lafayette, IN.

* Address correspondence to this author at: Department of Physics, Purdue University, West Lafayette, IN 47907. Fax: 765-494-0706; e-mail nolte@physics.purdue.edu.

Received May 1, 2006; accepted August 30, 2006.

Previously published online at DOI: 10.1373/clinchem.2006.072793

⁴Nonstandard abbreviations: BioCD, biological compact disc; PSI, poly-succinimide; PBS, phosphate-buffered saline; BSA, bovine serum albumin.

ASSAY PRINCIPLE

The BioCD is based on the principle of optical interferometric detection in the condition of phase quadrature, in which interference intensity depends linearly, and with maximum sensitivity, on small phase differences in the signal beam. Phase modulation on the BioCD is caused by the presence of bound mass on the reflective surface of a disc. The differentiation between specifically and nonspecifically bound mass is accomplished by differencing side-by-side target and reference protein spots. The key to the stable interferometric performance on a rapidly spinning disc is the local generation of both the signal and reference beams at the protein pattern. Mechanical vibrations are common to both beams and hence cancel, a process called self-referencing, or common-path, interferometry. Several methods exist of achieving self-referencing interferometry in the quadrature condition on a rapidly spinning disc. We have already demonstrated microdiffraction quadrature (4) and adaptive optical quadrature (5). In this study, we describe differential phase contrast scanning as a means of achieving quadrature detection of proteins on a spinning disc.

AQ: F

F1

The principle of differential phase contrast detection is shown in Fig. 1. The focused laser is diffracted by the edge of the printed protein and is Fourier transformed by the objective lens to the Fourier plane. The fields from the "land" (reference surface) and from the protein are 90° out of phase and hence in the quadrature condition at 2 quadrature angles, defined by the following equation:

$$\theta_Q = \pm \sin^{-1} \left(\frac{\lambda}{2w_0} \right), \quad (1)$$

where w_0 is the full width of the focused beam. The changes in intensities caused by the protein are equal and opposite at these angles. A split photodetector at the Fourier plane produces a signal equal to the difference between the 2 halves. This signal is proportional to the height of the printed protein. When the disc spins, the laser spot successively samples the leading and trailing edge of the protein. An example of the data generated from the photodetector as the laser spot traverses a series of patterned antibody monolayer "spokes" (~5 nm high and 100 microns wide) is shown in Fig. 2. The phase channel detects the edges of the protein, whereas an amplitude channel collects all the light and monitors light scattering and attenuation, which are negligible in these data. The small fluctuations in the phase-channel data are not noise but are actual surface structures that can be measured repeatedly. The leading edge of the protein spoke produces a positive signal and the trailing edge produces a negative signal. In the phase channel, the photodetector signal is proportional to the derivative of the surface height profile. The experimental conversion factor from the data is ~1.7 mV/nm for a detector full scale of 1.2 V. Because the thickness of a bilayer depends on the cube root of the molecular weight, the interfero-

F2

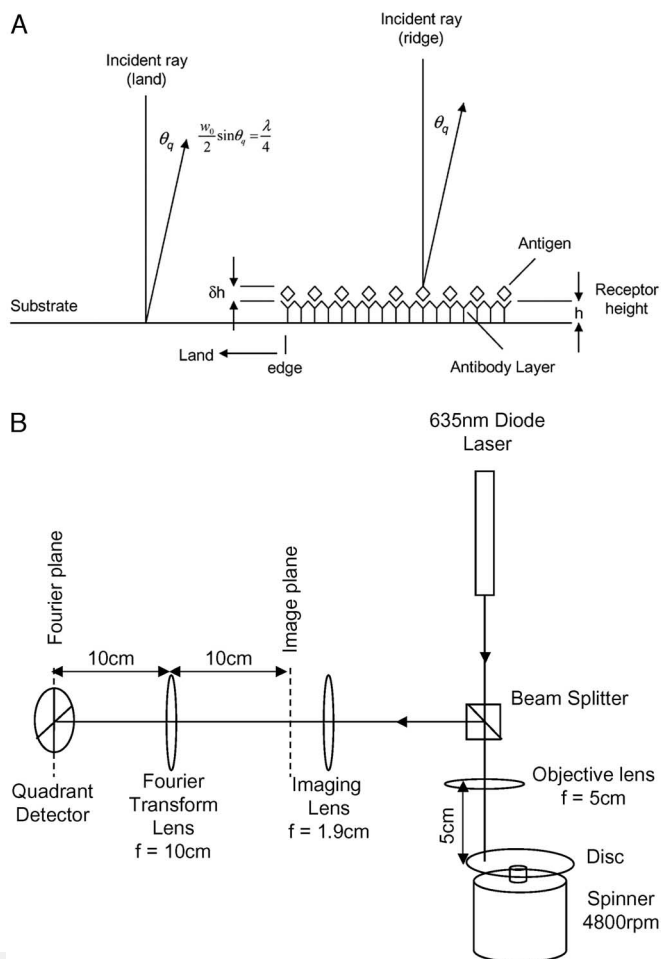


Fig. 1. (A), principle of differential phase contrast detection. A focused incident gaussian laser beam with diameter w_0 is diffracted by a protein edge into the far field.

At the quadrature angle, θ_q , the diffracted field from the land and the protein has the quadrature condition, which converts surface height (specifically surface electric dipole density) to amplitude at the detection plane. (B), a schematic drawing of the far-field optical detection system showing the Fourier transform lens and split detector in relation to the disc and incident laser illumination.

metric sensitivity falls only slowly with the size of the protein.

Materials and Methods

The phase-contrast BioCDs are fabricated from 100-mm diameter 1.1-mm thick borosilicate glass disks coated with a 10-layer dielectric stack of $\text{Ta}_2\text{O}_5/\text{SiO}_2$ that serves as a mirror with a center wavelength at 635 nm. The final layer is a $\lambda/4$ layer of SiO_2 , onto which protein patterns are immobilized through several different chemical approaches. We have used 3 standard protein immobilization techniques: physical adsorption through silanization of the silica surface (6), covalent biotin-avidin binding for high-affinity immobilization, and covalent binding to a surface of (3-aminopropyl)triethoxysilane (7) that had been conjugated with poly(ethylene glycol) diglycidyl ether. With physical adsorption, our silanization followed

AQ: G

AQ: H

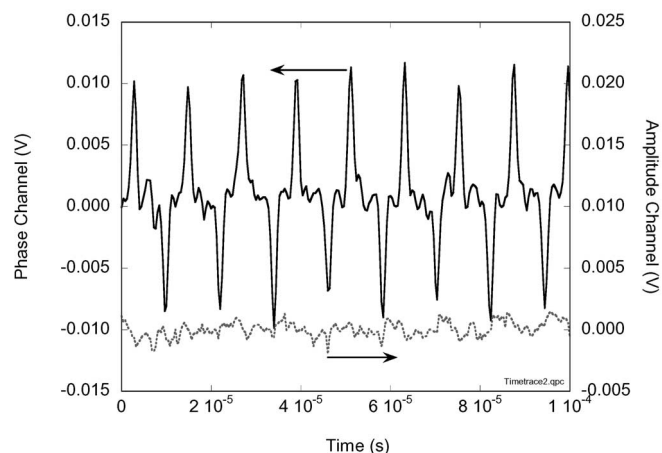


Fig. 2. Data collected from the split photodetector when the laser spot scans across consecutive avidin/biotin-antirabbit IgG protein spokes. The phase channel gives the differences in detected intensity between the 2 halves, whereas the amplitude channel collects the total intensity and monitors scattering.

a standard protocol in which the silica surface is soaked in 0.01 mol/L chlorodimethyloctadecylsilane in toluene for 16 h. Proteins bind through hydrophobic interaction with the organic end groups. Patterning of the protein in this case is accomplished by a gel stamp method. A polyacrylamide gel stamp infused with protein at a concentration of 10 mg/L in 1.5 mol/L Tris-HCl buffer at pH 8.8 is brought into contact with the surface. Protein diffuses from the gel onto the surface, where it is captured.

In the 2 covalent approaches, protein is patterned by photolithography. In the biotin-avidin approach the surface is coated with a polysuccinimide (PSI) polymer that is conjugated with biotin. After photolithography, the exposed surface is treated with avidin. Biotinylated antibodies are then added at a concentration of 10 mg/L in 10 mmol/L phosphate-buffered saline (PBS), pH 7.4; the antibodies attach to the avidin in the exposed regions. In the 3-aminopropyltriethoxysilane approach, the disks are patterned with photolithography, and the exposed area is passivated by 1% sodium borohydride solution. The photoresist is removed with acetone, and capture protein is applied at a concentration of 10 mg/L in 10 mmol/L PBS, pH 7.4, and binds covalently to the surface.

The optical detection system of the phase-contrast BioCD is simple, as shown in Fig. 1B. A 635-nm diode laser is focused onto the disc by a 5-cm focal length objective, to a diameter of ~ 20 microns. The reflected and refracted light is collected by the same objective lens and directed toward a quadrant detector by a beam splitter. Two additional lenses are used to place the quadrant detector on the optical Fourier plane of the system. The quadrant detector has 3 output channels: the total intensity, the difference between top and bottom, and the difference between left and right. The first difference channel produces the desired phase signal, and diagnoses optical alignment and disc wobble. The amplitude chan-

nel provides information related to scattering losses from the disc.

A key role is played by the so-called land between the spokes of printed protein. This is the reference surface to which the protein signal (and more importantly the assay signal) is referenced. Very small changes in protein density are measurable because of the differential aspect of the interferometry, making $\sim 50\,000$ difference measurements per second between protein and land as the disc spins. The high sampling rate and differential measurements allow detection of protein mean height changes down to tens of picometers (1 picometer = 1/1000th of a nanometer). The corresponding minimum detectable mass within the size of the laser spot is a few femtograms.

To obtain a response curve as a function of analyte concentration in the sample, we shifted to a different disc layout that used spots arranged in a regular grid. The disc was printed with mouse IgG (Sigma) and rabbit IgG (Sigma) spots deposited at 300 pL per spot by a high-speed protein printer (Scienion, Inc.). The resulting spot diameters were ~ 100 microns. The spotting removed the need for protein patterning but still provided many high-speed differential interferometric measurements between protein and land. More than 3000 spots were printed on a disc in groups of 4, called unit cells, that had 2 rabbit and 2 mouse IgG antigen spots each. The precise locations of the spots were referenced relative to a fiducial mark on the rim of the disc. In this experiment, the entire disc was incubated against increasing mouse antibody concentration in 10 $\mu\text{g/L}$ casein, 0.05% Tween 20, and 10 mmol/L PBS buffer for 20 h on an orbital shaker. This long-duration incubation protocol ensured equilibrium conditions with no mass transport limitations. The printed spots were analyzed by taking the difference between the printed mouse and rabbit spots. The difference was subtracted in each unit cell, which provided an accurate method for subtracting common binding to both sets of spots.

Results and Discussion

Examples of phase-contrast scans are shown in Fig. 3. The track pitch (spacing between tracks) is 20 μm with a laser spot diameter of 20 μm . In Fig. 3A, bovine serum albumin (BSA) was printed in parallel ridges ~ 100 microns wide by the gel-stamp method on a silanized surface. Apparent bending of the ridges is caused by an offset between the center of the printed pattern and the spin axis of the disc. In Fig. 3B, avidin protein was printed by photolithography onto a biotinylated PSI surface. The grayscale displays the derivative of protein height (more technically, the derivative of surface electric dipole density). The protein patterns in Fig. 3A are approximately monolayers of IgG. Note that the leading edge is bright and the trailing edge is dark, corresponding to the step-up and step-down from the printed protein.

A binary assay was performed on a gel-printed disc that tested for specific vs nonspecific binding and against

AQ: N

AQ: O

AQ: P

F3

AQ: Q

AQ: R

AQ: S

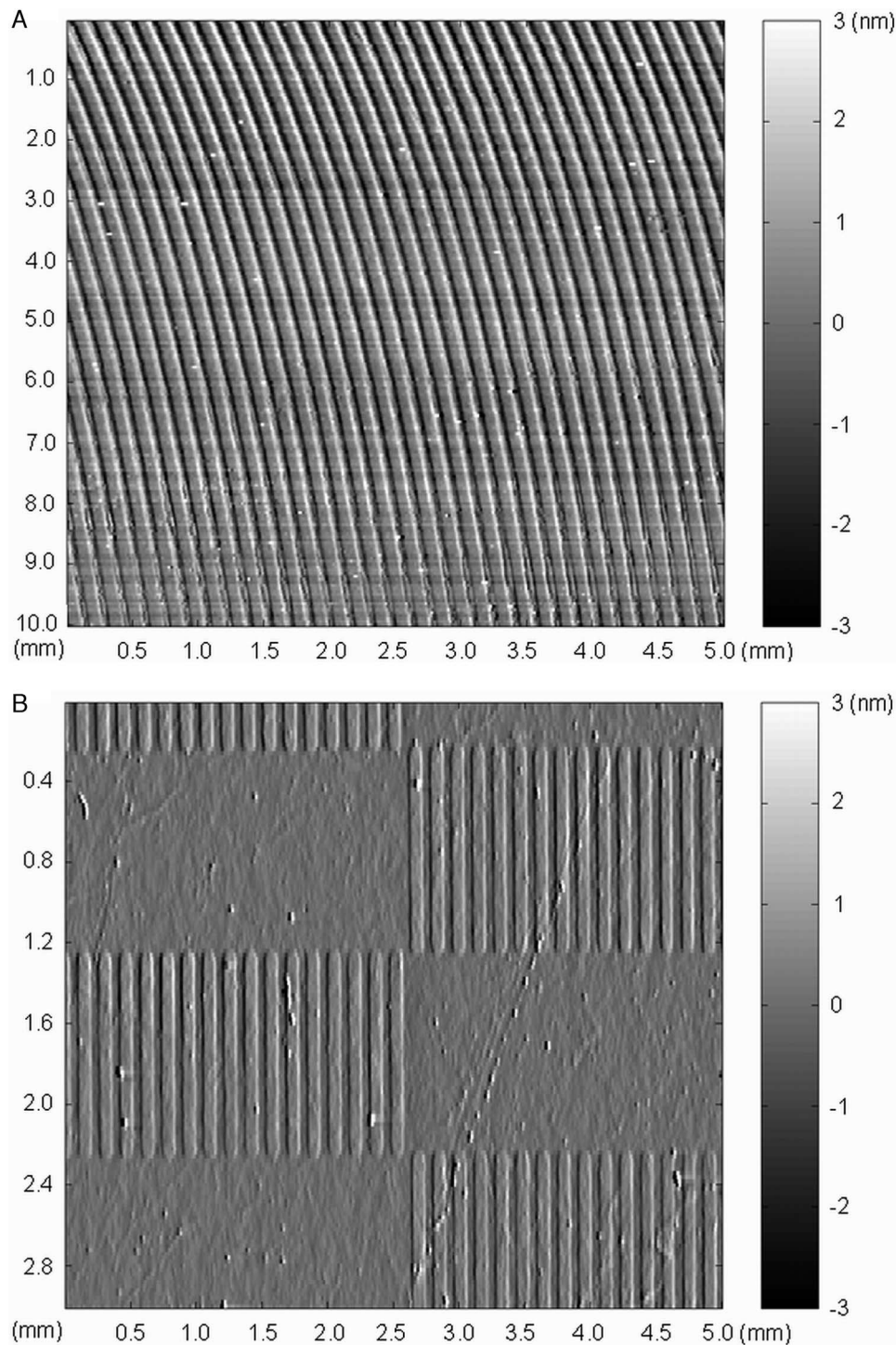


Fig. 3. Examples of phase contrast scans.

(A), scan on a disc patterned with BSA by the gel printing technique. The apparent warping of the ridges is because the ridge pattern was not concentric to the spin axis. (B), scan on a delectric disc patterned by photolithography with avidin on biotinylated PSI. Sizes of the scans are in millimeters.

AQ: T

F4

a negative control, the layout of which is shown in Fig. 4A. The disc was first patterned uniformly with the gel-stamp method with 100-micron-wide BSA ridges on silanized land. A duty cycle of $\sim 50\%$ was attained by the use of 1024 ridges around the disc. The surface of the disc was divided into 4 quadrants that were backfilled separately with 10 mg/L horse IgG (Sigma), BSA, mouse IgG (Sigma), and PBS, respectively, by use of multiple dis-

penses from a pipette to cover each quadrant. In the incubation process, the disc was incubated in 2 radial bands of antimouse IgG from goat serum (Sigma), and antihorse IgG from rabbit serum (Sigma); a 3rd, central band was not incubated. We used a pipette to dispense the incubation solution onto the disc in arc-shaped pools, taking care to prevent the pools from merging. This layout had 2 specific reactions (antihorse on horse and antimouse

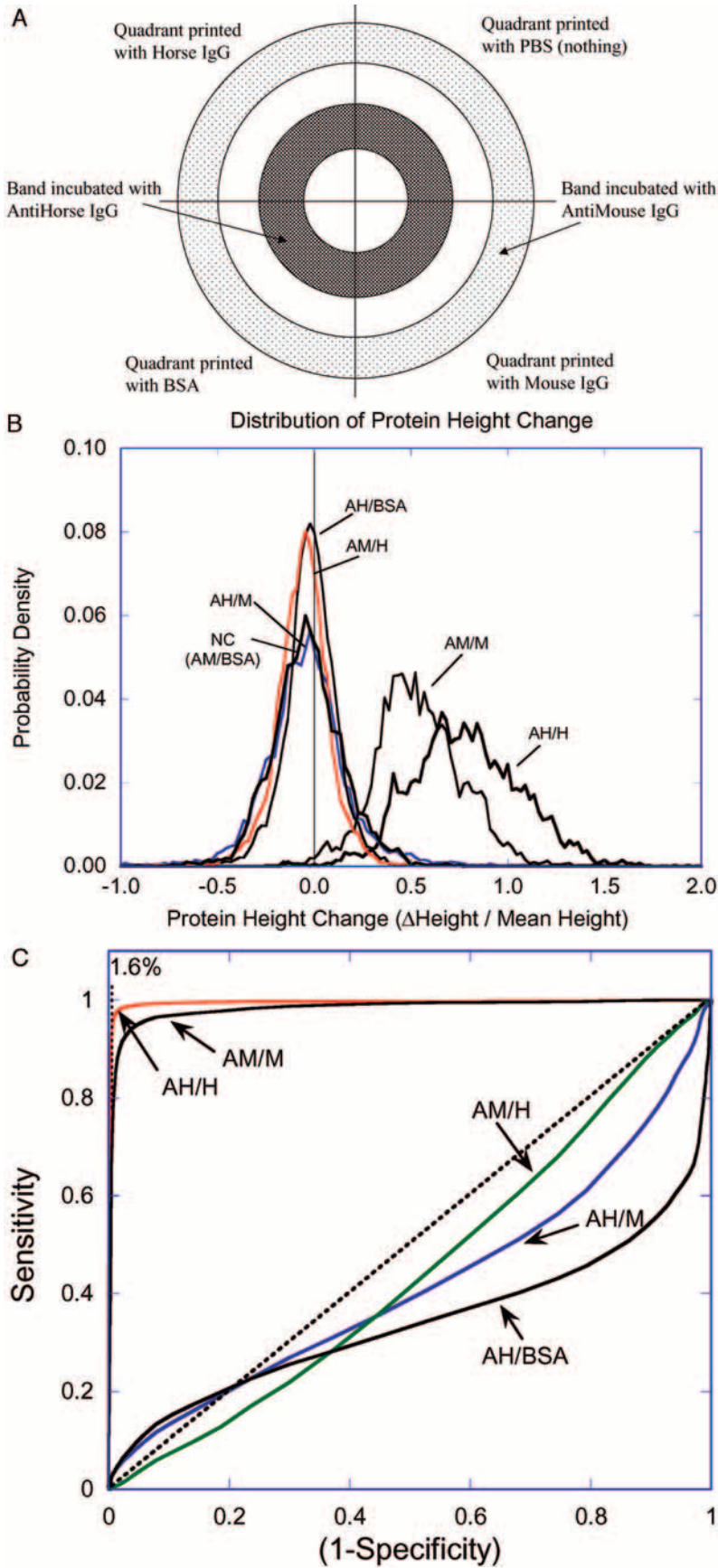


Fig. 4. (A), the disc layout of the binary assay experiment with horse or mouse IgG antigen immobilized in 2 quadrants, with BSA and bare disc on the other 2 quadrants.

The disc was incubated against antihorse antibodies on the inner band and against antimouse antibodies on the outer band, both at 10 mg/L for 30 min. (B), histograms of protein height change after the incubation with antibodies. AH/H, antihorse against horse; AM/M, antimouse against mouse; AH/BSA, antihorse against BSA; AM/H, antimouse against horse; AH/R, antihorse against rabbit; NC, the negative control (antimouse against BSA). (C), the resulting ROC of the IgG assay at 10 mg/L. Specific assays behave as a step function, whereas nonspecific and cross-reactivity assays are close to the diagonal line. When true positive is at 98%, the false positive is <2%.

on mouse), 2 cross-reactivity reactions (antihorse on mouse and antimouse on horse), and 2 negative controls (antihorse against BSA and antimouse against BSA). One of these negative controls, the antimouse on BSA, was used to define the specificity of the assay. The sample concentrations of target for the binary assay were 10 mg/L incubated in PBS buffer for 30 min.

The results of the assay are shown in a histogram of protein height change after antibody incubation in Fig. 4B. The 2 specific assays (antimouse/mouse and antihorse/horse) show clear separation from the cross-reactivity and negative control results, with large mass binding between 50% and 100% of the printed protein. The histograms were used to construct the ROC graph in Fig. 4C. The horizontal axis is 1 minus the specificity of the assay, defined by the cumulative area under the histogram of antimouse/BSA in Fig. 4B. The vertical axis is the sensitivity, defined by the cumulative area under the other histograms. The 2 cross-reactivity assays follow a nearly diagonal trace on the graph, as expected, whereas the 2 specific assays are nearly step functions. For the specific assays, both the false positives and the false negatives were <2% at 10 mg/L.

F5

The response curve as a function of analyte concentration in the sample is shown in Fig. 5. The response is plotted in units of mass gained per spot against the concentration of specific analyte. The error bars on the graph are statistical, based on the mean over the entire set of spots on the disc. Also included is a smooth fit to a stretched response function modeled by an exponential distribution of k_a values for the bound antigen vs free antibody reaction. The wide distribution of k_a is consistent

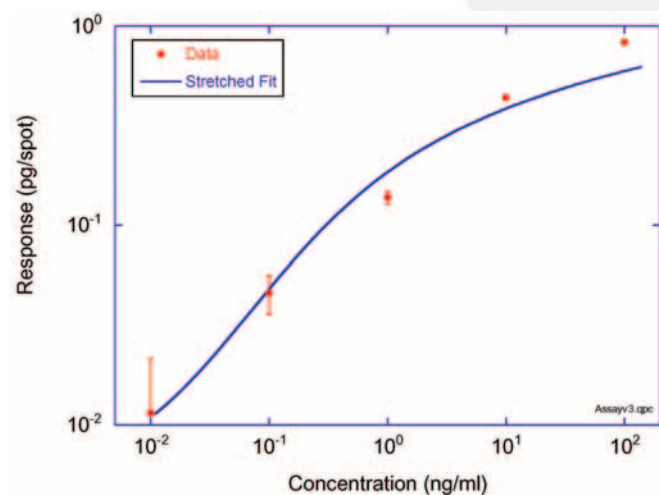


Fig. 5. Dose-response curves of a 3000-spot mouse and rabbit IgG reverse assay expressed as mass bound per spot.

A single disc was incubated against successively higher concentrations. The smallest resolvable mass change was 10 fg/spot, with a mean mass per spot of 10 pg. The fit is a phenomenologic stretched response that assumes a wide distribution in k_a values.

with protein denaturation on immobilization. The sensitivity limit of the assay is ~ 100 ng/L, corresponding to a mass difference of only 10 fg/spot. These results can be used to scale the results to different numbers of spots per assay by the assumption that the signal-to-noise ratio of the measurement scales according to Poisson statistics as the square root of the number of spots. For instance, because $\sqrt{3000} = 50$, we can extrapolate that a single antigen spot would have a detection limit of 5 $\mu\text{g/L}$ of antibody for an equilibrium assay. The high sensitivity of this last assay represents a best-case condition in which sample volume and analyte transport were not limiting factors. In real applications in diagnostic medicine, on the other hand, sample volume and analyte transport are often limiting factors, but the results here provide a starting point for understanding the assay sensitivities under these conditions.

Considerable improvements in the disc preparation will be possible in the future. The most important improvement will be to increase the fraction of biologically active immobilized protein molecules. Improvements in surface chemistry and disc preparation may be expected to improve the fraction of biologically active immobilized molecules. Other areas open to improvement include uniform k_a distributions, decreased nonspecific binding affinities, better surface passivation, and higher spot uniformity. Gains in each of these will improve the assay detection limits.

This work was performed through a sponsored research grant through the Purdue Research Foundation from QuadraSpec, Inc.

References

1. Varma M, Nolte DD, Inerowicz HD, Regnier FE. High-speed label-free multi-analyte detection through micro-interferometry. In: Nicolau DV, Raghavachari R, eds. *Microarrays and Combinatorial Technologies for Biomedical Applications: Design, Fabrication, and Analysis*. SPIE 2003;4966:58–64.
2. Varma MM, Nolte DD, Inerowicz HD, Regnier FE. Spinning-disk self-referencing interferometry of antigen-antibody recognition. *Opt Lett* 2004;29:950–2.
3. La Clair JJ, Burkart MD. Molecular screening on a compact disc. *Org Biomol Chem* 2003;1:3244–9.
4. Varma MM, Inerowicz HD, Regnier FE, Nolte DD. High-speed label-free detection by spinning-disk micro-interferometry. *Biosens Bioelectron* 2004;19:1371–6.
5. Peng L, Varma M, Inerowicz HD, Regnier FE, Nolte DD. Adaptive optical BioCD for biosensing. *Appl Phys Lett* 2005;86:183902–1–3.
6. Dutchet BCJ, Chapel JP, Gérard JF, Chovelon JM, Jaffrezic-Renault N. Influence of the deposition process on the structure of grafted Alkylsilane Layers. *Langmuir* 1997;13:2271–8.
7. Qian W, Yao D, Xu B, Yu F, Lu Z, Knoll W. Atomic force microscopic studies of site-directed immobilization of antibodies using their carbohydrate residues. *Chem Mater* 1999;11:1399–401.